# Data-efficient machine learning potentials from transfer learning of periodic correlated electronic structure methods: liquid water at AFQMC, CCSD, and CCSD(T) accuracy

Michael S. Chen, <sup>1</sup> Joonho Lee, <sup>2</sup> Hong-Zhou Ye, <sup>2</sup> Timothy C. Berkelbach, <sup>2,3,a)</sup> David R. Reichman, <sup>2,b)</sup> and Thomas E. Markland <sup>1,c)</sup>

(Dated: 28 April 2023)

Obtaining the atomistic structure and dynamics of disordered condensed phase systems from first principles remains one of the forefront challenges of chemical theory. Here we exploit recent advances in periodic electronic structure and provide a data efficient approach to obtain machine learned condensed phase potential energy surfaces using AFQMC, CCSD, and CCSD(T) from a very small number (≤200) of energies by leveraging a transfer learning based scheme starting from lower tier electronic structure methods. We demonstrate the effectiveness of this approach for liquid water by performing both classical and path integral molecular dynamics simulations on these machine learned potential energy surfaces. By doing this we uncover the interplay of dynamical electron correlation and nuclear quantum effects across the entire liquid range of water while providing a general strategy for efficiently utilizing periodic correlated electronic structure methods to explore disordered condensed phase systems.

#### I. INTRODUCTION

Ab initio molecular dynamics (AIMD) simulations, where the forces and energies are generated at each time-step by performing an electronic structure calculation, provide an appealing route to simulate reactive chemical dynamics. However, for disordered condensed phase systems an accurate description typically requires many 100's of atoms to obtain a chemically reasonable description of bulk systems (e.g., water) and this grows into the 1000's for more heterogeneous systems (e.g., those with interfaces). Since AIMD simulations require an electronic structure calculation to be performed at each time-step, to statistically converge even simple thermodynamic properties necessitates many tens of thousands of ab initio calculations (10's of picosecond timescale at a  $\sim 1$  fs time step) and for slower converging properties many millions are needed (nanosecond timescale). The computational expense of these simulations is further compounded if one wants to incorporate nuclear quantum effects (NQE) via ab initio path integral molecular dynamics simulations (PIMD). Due to its reasonable compromise between accuracy and efficiency, density functional theory (DFT) is currently the most frequently employed electronic structure method in condensed phase AIMD studies. However, the results depend—sometimes sensitively—on the choice of the exchange-correlation functional and the inclusion of dispersion corrections.<sup>1,2</sup> This issue motivates the use of beyond-DFT electronic structure theories, such as those based on the many-electron wavefunction. For example, work performed almost a decade ago demonstrated the AIMD simulations of liquid water using second-order Möller-Plesset perturbation theory (MP2).<sup>3</sup> However, the high cost of more accurate methods precludes their direct use in AIMD.

Machine learned potentials (MLPs) have emerged as an extremely promising approach to accurately model ab initio potential energy surfaces of condensed phase systems while being orders of magnitude more computationally efficient to evaluate. For liquid water, MLPs have been successfully developed at various levels of electronic structure ranging from different levels of DFT<sup>4-10</sup> to more recently using the random phase approximation (RPA)<sup>11</sup> and MP2.<sup>12,13</sup> The modeling of liquid water and other molecular systems with more accurate electronic structure methods, such as coupled-cluster theory or quantum Monte Carlo, has been so far limited to training on finite clusters of molecules. 14-26 When training on small clusters, higher-order many-body interactions have to be included by other means such as by using the TTM4-F potential<sup>27</sup> as is done for the MB-Pol water model. 15-18 Other clusterbased models for water have gone on to explicitly include 4-body terms<sup>20-22</sup> and also train on larger water clusters.<sup>23</sup> MLPs fit to periodic electronic structure offer the opportunity to readily capture many-body electronic structure effects since these are naturally included in the electronic structure calculation. Recent advances have opened the door to efficiently calculating the properties of periodic condensed phase systems using higher-level methods like coupled cluster singles and doubles without and with perturbative triples (CCSD and CCSD(T))<sup>28,29</sup> and phaseless auxiliary-field quantum Monte Carlo (AFQMC).<sup>30</sup> However, while these advances allow the energies of many 100's of condensed phase configurations to be evaluated, this is still considerably less than what would be typically required to train an accurate MLP.

Here, we demonstrate that by using an approach based on transfer learning starting from a variety of lower tier electronic structure methods one can generate a highly data-efficient approach to training MLPs using high level electronic struc-

<sup>&</sup>lt;sup>1)</sup>Department of Chemistry, Stanford University, Stanford, California, 94305, USA

<sup>&</sup>lt;sup>2)</sup>Department of Chemistry, Columbia University, New York, New York 10027, USA

<sup>&</sup>lt;sup>3)</sup>Center for Computational Quantum Physics, Flatiron Institute, New York, New York 10010, USA

a)Electronic mail: t.berkelbach@columbia.edu b)Electronic mail: drr2103@columbia.edu

c)Electronic mail: tmarkland@stanford.edu

ture methods. With this approach, we show that only 200 high-quality energies obtained from small periodic boxes containing 16 water molecules provide sufficient data for training our MLPs. Specifically, we train MLPs to periodic electronic structure calculations performed with AFQMC, CCSD, and CCSD(T). The MLPs are then used to perform AIMD and PIMD simulations of larger water boxes for the long times necessary to statistically converge structural and dynamic properties using both classical and quantum mechanical treatment of nuclei. This allows us to achieve a careful comparison of the quality of the underlying electronic structure theories in describing water across its entire liquid temperature range and uncover the changes in the properties of liquid water as the dynamical electron correlation captured is increased. In addition, we provide a set of MLPs and a curated training set that can form the basis of future studies of water and aqueous systems. Our data-efficient approach provides a route to accurately obtain the properties of other disordered condensed-phase systems by combining high-level electronic structure theory and machine learning.

#### II. METHODS

### A. Machine learning

To develop a highly data efficient strategy that only requires a minimal number of energies from periodic high level electronic structure methods, such as CCSD, CCSD(T), and AFQMC, and produce accurate MLPs, we exploited a combination of approaches including an active learning procedure for curating a small but comprehensive training set, the training of MLPs to energies for small periodic boxes (16 waters) and showing that they reproduce properties when used for larger simulations (64 waters) and a transfer learning approach that leverages the transferability of physics from lower tier electronic structure methods.

# 1. Developing an efficient training set by leveraging a committee of machine learning potentials

We first applied an active learning procedure to curate a data efficient set of configurations to train our MLPs. We invoked the commonly employed Query-by-Committee (ObC)<sup>8,31,32</sup> approach to iteratively add configurations to the training set. At every iteration, the current dataset of configuration energies was used to train a committee of 8 MLPs, each a Behler-Parrinello neural network potential<sup>4,33</sup> with a different random initialization of weights and random trainvalidation (90-10) splits of the dataset. To mitigate overfitting, we applied early stopping to each of these MLPs in the committee, monitoring the energy prediction error over a validation set. The mean potential energy surface obtained for this committee MLP was used to run a short MD simulation (SI Sec. III) that was terminated either when the system becomes unphysical (i.e., reaching a temperature greater than 400K) or when 50 ps of simulation trajectory was generated. We then selected the 10 configurations where the committee MLP had the largest standard deviation in its potential energy prediction to recalculate at the target level of electronic structure theory and add to the training set for the next iteration of this procedure. To prevent selected configurations from being overly correlated with one another, no two selected configurations were closer than 100 fs apart. The initial dataset of 50 configurations used to initialize this procedure was also selected via an iterative QbC procedure, as applied to a single 100 ps SCC-DFTB<sup>34</sup> (SI Sec. III) trajectory, that started with 10 randomly selected configurations and added 10 additional configurations for each of 4 subsequent iterations.

We generated 5 different 200 configuration datasets by running 5 instances of our ObC active learning scheme where the target level of electronic structure theory was DFT using the revPBE0-D3<sup>35-37</sup> functional (SI Sec. IA) which was chosen due to being computationally efficient compared to the high level electronic structure methods and since it has previously been shown to produce the properties of liquid water accurately when combined with path integral simulations.<sup>38</sup> To select the generated dataset on which the higher tier electronic structure methods would be used we then used each of the 5 datasets to train a committee MLP using revPBE0-D3. We then selected the one that gave the lowest force prediction error (RMSE) when evaluated on a test set of 1000 water configurations (64 water molecules) drawn from previously published AIMD simulations.<sup>38</sup> To check the transferability of the selected 200 configuration dataset, we recalculated the energies and forces for the generated datasets and the test set using the BLYP<sup>39,40</sup> functional (SI Sec. I A). After training and evaluating a new set of BLYP trained MLPs, the same dataset that resulted in the lowest error revPBE0-D3 trained MLP also gave the lowest error BLYP trained MLP (SI Fig. 3). Given the transferability of the relative utility of this dataset, we used this same 200 configuration dataset to train our CCSD, CCSD(T), and AFQMC MLPs.

## 2. Training machine learned potentials on configurations of small systems

Given the significant scaling of CCSD, CCSD(T), and AFOMC's computational cost with system size, we sought to reduce the system size of the configurations used in our training set. We investigated the feasibility of training our committee MLP to the energies of a set configurations for small periodic boxes to accurately predict for properties associated with a larger simulation box. For liquid water running periodic molecular dynamics simulations of small water boxes (32 water molecules or fewer) leads to significant artifacts even in simple properties such as RDFs when compared to larger system sizes.<sup>41</sup> However, as demonstrated in SI Sec. VI for the revPBE0-D3 functional, if one trains a MLP on energies of small (16 molecule) periodic water configurations and then uses the resulting model to perform dynamics of a larger system (64 molecule), then the results obtained are in excellent agreement with those obtained from performing a AIMD simulation at the larger system size. Based on this demonstration

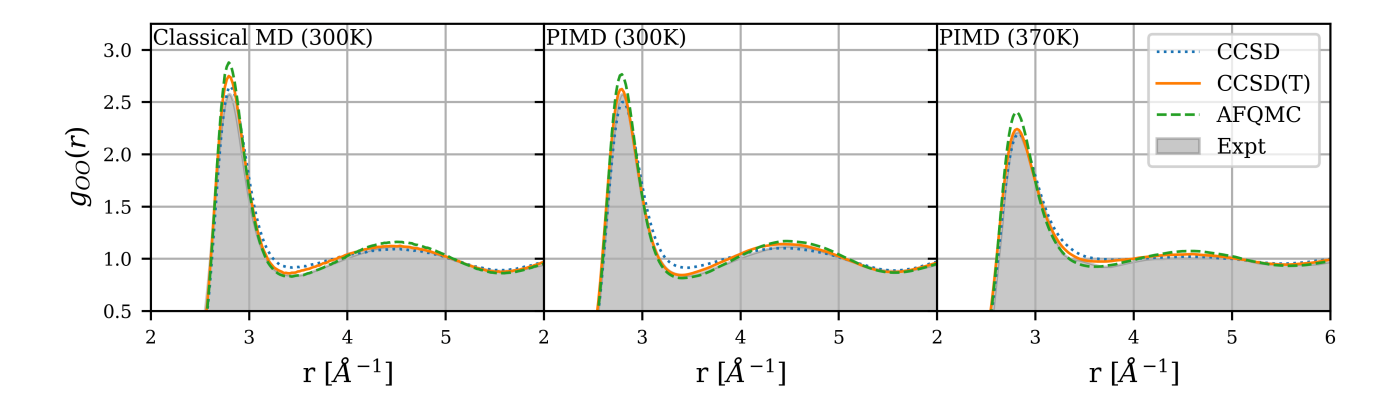


FIG. 1. Oxygen-oxygen RDFs for liquid water when running classical and PIMD simulations using NNPs fitted to either CCSD, CCSD(T), and AFQMC energies at both 300K and 370K. The PIMD oxygen-oxygen RDFs when using the CCSD(T) and AFQMC correspond closely with the experimental results shaded in grey at 295K and 366K.

we therefore trained the MLPs for the higher level methods on periodic configurations of 16 water molecules using the transfer learning approach described in the following section and then report the properties obtained in Sec. III by performing MD and PIMD simulations using 64 water molecules.

## 3. Transfer learning approach to train the MLPs

With only hundreds of energies from the higher tier periodic electronic structure methods available, to make efficient use of this data we employed a transfer learning approach.<sup>42</sup> To achieve this we first trained a committee MLP at a lower level of electronic structure theory, DFT or Hartree Fock (HF) on 531 configurations using both energies and gradients to improve the fitting. The parameters obtained for these MLPs were then used as the starting point for the fits to the higher level methods. This strategy exploits the idea that while the lower level methods may not reach the levels of chemical accuracy required for some applications they do contain fundamental physical information (e.g., about the fact that O and H when in close proximity form a high frequency chemical bond) that can be used to structure the neural network that underlies the MLP. Hence while the high level data is used to tune the accuracy of the MLP, it is leveraging the physics learnt by the initial training to the lower level method.

While using transfer learning to make efficient use of very small amounts of high level electronic structure data has distinct advantages over starting from a randomly initialized MLP, one must be mindful of the risk of hysteresis in the final MLP, i.e., that by biasing the weights by taking them from a model trained on a low level electronic structure method, that the final MLP will incorrectly contain remnants of the failures of the low level method. Hence to assess our transfer learning approach's ability to produce a final model that accurately reproduces the properties of the target high level electronic structure method, we initialized the procedure starting from a range of different low level methods that each give very different properties of liquid water. By comparing the

structural and dynamical properties of liquid water obtained by performing MD and PIMD simulations on the final models obtained from these different starting points, one can thus evaluate which properties are obtained universally across the models initialized from different low level methods and thus accurately reflect the high level electronic structure approach.

In practice, following the convergence of the lower level fits to both energy and gradient data (see SI Sec. II), we retrained the committee MLP (8 separate MLPs) to the energies of the higher level method employing the extended Kalman filter optimizer as implemented in the n2p2<sup>43</sup> package and using a 90-10 train-validation split in order to monitor the prediction error over the validation set for early-stopping each individual fit to prevent overfitting. Before applying this transfer learning approach to the high level CCSD, CCSD(T) and AFQMC methods for which AIMD is not possible for the timescales required, in SI Sec. VI we tested it by training an MLP with revPBE0-D3 as the higher level method and BLYP and HF as the lower level methods from which the transfer learning was performed and evaluated how well these resulting MLPs reproduced the properties obtained from revPBE0-D3 (SI Figs. 4-10). We chose DFT with the revPBE0-D3 exchange-correlation functional as the higher level in this benchmark due to its accurate description of the properties of liquid water and since we can compare the results of the transfer learned MLPs to AIMD and AI-PIMD trajectories that we have previously obtained.<sup>38</sup> We chose BLYP and HF as the lower level methods since the former gives an incredibly overstructured and dynamically sluggish description of water while the latter gives the opposite.

As shown in SI Sec. VI, MD simulations using the final transfer learned MLP models of revPBE0-D3 using only 200 energies starting from either BLYP or HF correctly capture the target RDFs and VDOS for liquid water at 300K obtained from AIMD simulations, which are both markedly different from those given by low level methods themselves (BLYP water has a more structured oxygen-oxygen RDF and higher wavenumber hydrogen VDOS bend and stretch peak positions than revPBE0-D3 water, and vice-versa for HF water). The

agreement with the reference revPBE0-D3 results for both models is particularly strong for the RDFs. For the VDOS, the BLYP-initialized model outperforms the HF-initialized model in capturing the high frequency O-H stretch peak. Both models also accurately reproduce the RDFs obtained from AI-PIMD simulations of revPBE0-D3 for liquid water<sup>38</sup> at 300K (SI Fig. 5) with the only discrepancy again being in the VDOS (SI Fig. 10) where the BLYP-initialized MLP captures the full spectrum whereas HF shows an overstructured and blue shifted OH stretch region.

Additionally, we compared our transfer learning approach to two common alternative machine learning approaches: directly training a committee MLP on the high level energies starting from randomly initialized weights and training a committee delta-learning model that corrects from the lower to higher level method. To allow for a fair comparison, all three types of models were trained to the same 200 configuration training set of energies (revPBE0-D3) for liquid water using the same MLP architecture and optimization settings. The randomly initialized model resulted in a potential that was unstable for the purposes of running MD for a periodic simulation box of 64 water molecules, with the instantaneous temperature drifting severely after the first simulation step. For the delta-learning model, we trained a committee MLP to capture the energy difference between revPBE0-D3 and another committee MLP trained to BLYP. The delta-learning model was similarly as unstable as the randomly initialized model. Hence for liquid water with 200 energies at the higher level we found that the transfer learning approach we have detailed above provides the most accurate results.

Given the demonstrated efficacy of our transfer learning procedure, in Sec. III we applied this approach to train committee MLPs to CCSD, CCSD(T), and AFQMC energies for liquid water using three different sets of MLP initializations: HF, BLYP, and revPBE0-D3.

## B. Correlated electronic structure methods

We perform correlated electronic structure calculations of liquid water with periodic boundary conditions at the Γ-point using AFQMC, CCSD, and CCSD(T). Periodic CCSD and CCSD(T) calculations were performed using PySCF<sup>44,45</sup> where electron-repulsion integrals are handled using the range-separated density fitting method, 46,47 and AFQMC calculations were performed using QMCPACK<sup>48,49</sup> and ipie. 50 These calculations all began with a periodic spin-restricted HF calculation also performed using PySCF. We provide brief details here, and further information can be found in SI Secs. I B and I C.

AFQMC is a projector Monte Carlo method where the ground state of a given Hamiltonian is obtained via imaginary time evolution. Without any approximations, it scales exponentially as the system size grows due to the fermionic sign problem. We use the phaseless approximation<sup>30</sup> to obtain an algorithm that scales with the system size N as  $O(N^3) - O(N^4)$  for each sample at the expense of introducing errors in the final ground state energy estimate. The phaseless approxi-

mation sets a boundary condition in imaginary time evolution using a priori chosen wavefunction called the trial wavefunction. The bias from this approximation becomes smaller as one improves the quality of trial wavefunctions. In this work we employ the simplest trial wavefunction, the spin-restricted Hartree-Fock determinant. A recent benchmark study examined the accuracy of AFQMC with Hartree-Fock trial wavefunctions over 1004 data points, <sup>51</sup> and based on these results at this level of approximation we expect the accuracy of AFQMC to be between CCSD and CCSD(T) for the problems considered here.

Coupled cluster (CC) parameterizes the electronic wavefunction using an exponential ansatz,  $|\Psi_{CC}\rangle = e^{\hat{T}} |\Phi_{HF}\rangle$ , where  $\hat{T}$  creates all possible particle-hole excitations from the HF reference and is determined by iteratively solving a set of coupled non-linear equations.<sup>52</sup> CCSD approximates the full CC ansatz by truncating the T-operator at single and doubleexcitation levels,  $\hat{T} = \hat{T}_1 + \hat{T}_2^{28}$  CCSD(T) improves upon CCSD by further including the contribution from triple excitations in a perturbative (non-iterative) manner<sup>29</sup> and is often referred to as the "gold standard" in the quantum chemistry of simple molecules. The computational cost of CCSD and CCSD(T) scales more steeply than that of AFQMC, as  $O(N^6)$ and  $O(N^7)$ , respectively. In this work, we avoid the high computational cost of full CCSD and full CCSD(T) by systematically compressing the virtual space using the frozen natural orbital (FNO) approximation, <sup>53,54</sup> which we confirmed to introduce a negligible error (SI Sec. IB).

#### III. RESULTS AND DISCUSSION

Having established the applicability of our data efficient approach to training MLPs that accurately reproduce the target potential energy surfaces on DFT, we now apply it to obtain the structural and dynamic properties of liquid water using three correlated methods: CCSD, CCSD(T), and AFQMC. We trained a committee MLP, which as described in Sec. II A 1 is formed of the mean of 8 independently trained MLPs, for each correlated electronic structure method. By performing MD and PIMD simulations in the NVT ensemble at 300 K and 370 K using the committee MLP for each electronic structure method, here we evaluate how different treatments of dynamical electron correlation affect the selected properties when the nuclei are treated classically or quantum mechanically.

To provide an assessment of the accuracy of our transfer learned committee MLPs on different structural and dynamical properties as discussed in Sec. II A 3 we can compare the consistency of the results obtained from models that have been initially trained to different lower level electronic structure methods. Hence, for each of the correlated methods we trained three transfer learned committee MLPs starting from HF, BLYP, and revPBE0-D3 as our lower level methods which are known to understructure, overstructure, and accurately reproduce the properties of water respectively. Performing classical MD at 300K from MLPs starting from these three different methods SI Fig. 13 shows that regardless of the lower

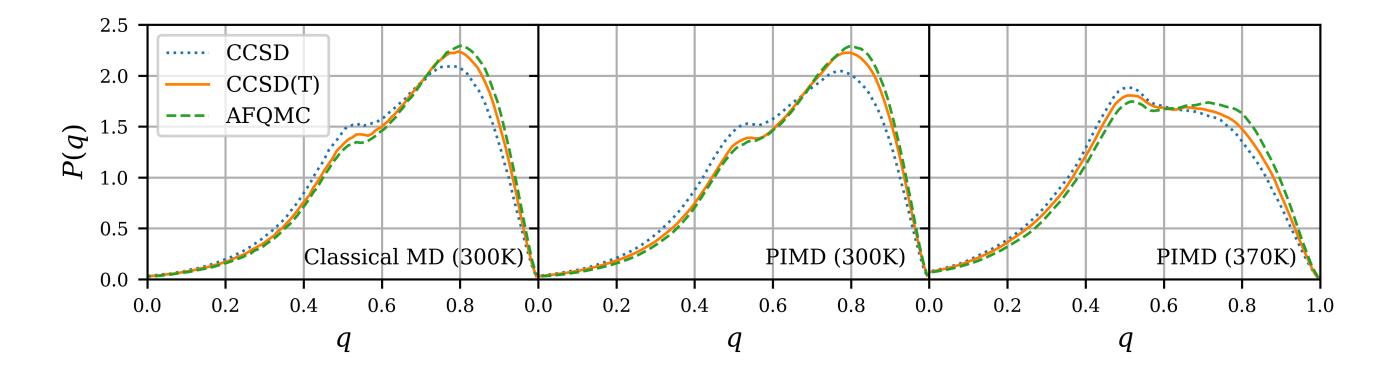


FIG. 2. Tetrahedral order parameter *q* distributions as sampled via classical and PIMD simulations via NNPs fitted to either CCSD, CCSD(T), and AFQMC energies at both 300K and 370K.

level that the transfer learning was initialized with, the properties obtained at the high level, AFQMC in this case, coincide closely although the O-H stretch for the HF-initialized model is blue-shifted slightly. This demonstrates that our training set of 200 energies of periodic boxes consisting of 16 water molecules is large and diverse enough to train an accurate model of liquid water under these conditions using our transfer learning protocol. When nuclear quantum effects are included by peforming PIMD simulations using the committee MLPs, the oxygen-oxygen RDF and VDOS for the revPBE0-D3 and BLYP initialized transfer learning models remain consistent with one another (SI Fig. 14).

In this section we show the results from the committee MLP generated using transfer learning from revPBE0-D3 for each of the correlated methods since, as shown in SI Fig. 2, revPBE0-D3 shows the strongest correlation with the training set energies of CCSD, CCSD(T), and AFQMC out of the three initialization methods we used (HF, BLYP, and revPBE0-D3). We note that the AFQMC and CCSD(T) energies computed in this work and their correlations with other methods in SI Fig. 2 can also be used to provide a benchmark for electronic structure methods in the condensed phase. By comparing all the other methods' energies to those from AFQMC one observes the following strength of correlations: CCSD(T) > CCSD > revPBE0-D3 > MB-Pol > BLYP > HF. For the other high tier electronic structure method used here, CCSD(T), a similar trend is observed: CCSD > AFQMC > revPBE0-D3 > MB-Pol > BLYP > HF.

For our AFQMC results, it is important to note that the AFQMC energies contain stochastic error, with each of our N=200 training set AFQMC energies having a corresponding estimate for the standard error that ranges from 1-2 mH depending on the specific training set configuration. To evaluate how this level of error might affect our reported properties, we employed a test where we sample new training sets where the same N=200 configuration are used but a random value is added to each AFQMC energy to reflect the uncertainty of our AFQMC energies (see SI Sec. VII for details). In total, 12 training sets were sampled and a transfer learned committee MLP was fit to each. SI Figs. 11 and 12 serve to quantify the variations in the oxygen-oxygen RDF and hydrogen VDOS

obtained from the 12 separate training sets due to the stochastic error in the AFQMC energies, with the grey shading representing the standard deviations. From this test we found that the stochastic error in our AFQMC calculations does introduce noticeable variations in the OH stretch peak of the hydrogen VDOS, particularly around the top of the peak, but the RDFs and VDOS are otherwise consistent for the different training sets.

## A. Structural properties of water from correlated electronic structure methods

We first compare the structural equilibrium properties for liquid water at 300 K and 370 K obtained via classical MD and PIMD simulations using the committee MLP for each correlated electronic structure method. For these properties PIMD exactly includes the NQEs for distinguishable particles, which is a highly reliable assumption for nuclei at this temperature. Figure 1 shows the oxygen-oxygen RDFs for each of CCSD, CCSD(T), and AFOMC as compared to the experimental results at 295 K<sup>55</sup> and 366 K.<sup>56</sup> At 300 K, classical MD CCSD(T) and AFQMC both give a first peak that is slightly higher than observed experimentally suggesting the liquid is overstructured. However, once NQEs are accounted for in the PIMD simulations both RDFs become slightly less structured and show better agreement with experiment, with that of CCSD(T) coinciding quantitatively. CCSD gives good agreement with experiment when used in classical MD simulations but is understructured when NQEs are included which is consistent with this electronic structure approach starting from a HF reference which gives a severely understructured liquid with the additional dynamical correlation added through the tiers of CC theory progressively structuring the liquid. At 370 K when used in PIMD simulations all methods give good agreement with the experiment with AFQMC again exhibiting a first peak that is higher than CCSD, CCSD(T) and experiment. SI Fig. 15 and Fig. 16 show the hydrogen-hydrogen and oxygen-hydrogen RDFs at 300 K sampled via classical MD and PIMD, respectively, where all three electronic structure methods give similar results but AFQMC again exhibits a more structured hydrogen bond network with the first intermolecular OH peak at  $\sim$ 1.85 Å, which corresponds to hydrogen bonds, being slightly higher than the other methods.

The tetrahedral order parameter provides a measure of higher order structural correlations within water's hydrogen bond network beyond the purely radial information encoded in the RDFs. The tetrahedral order parameter q is defined for a given water molecule as,  $^{57}$ 

$$q = 1 - \frac{3}{8} \sum_{j=1}^{3} \sum_{k=j+1}^{4} \left( \cos \theta_{jk} + \frac{1}{3} \right), \tag{1}$$

where  $\theta_{jk}$  is the angle that a given water molecule's oxygen atom makes with two neighboring oxygen atoms j and k. The tetrahedral order parameter thus ranges from 0 to 1 with higher values indicating that the hydrogen bond network possesses angles closer to that of a perfect tetrahedral arrangement of the four nearest neighbour oxygen atoms around a central water molecule. As shown in Fig. 2 at 300 K for both classical MD and PIMD this property further highlights the understructured hydrogen bond network of CCSD compared to the more accurate correlated methods, CCSD(T) and AFQMC, that are in close agreement. At 370 K the distribution of the tetrahedral order parameter for all three methods shifts to lower values.

The comparison of these structural equilibrium properties suggests that the inclusion of higher order electron correlation contributions in methods like CCSD(T) and AFQMC, as compared to CCSD or HF, results in a greater degree of structuring in liquid water at 300 K and 370 K. Given the directional nature of this additional structuring, as seen from the greater probability density at higher q in Figure 2, this arises from slightly stronger hydrogen bonds being formed when using the two higher level methods. Our comparisons of the oxygen-oxygen RDFs obtained from classical and PIMD simulations at 300 K also show that for these correlated methods the inclusion of NQEs works to slightly destructure liquid water. The relatively subtle overall effect of NQEs on liquid water around 300 K is known to arise from the close balance of competing quantum effects in this system.<sup>58</sup>

# B. Dynamical properties of water from correlated electronic structure methods

We now turn our attention to how the different correlated electronic structure methods behave when used to compute dynamical properties of liquid water, namely the self diffusion coefficient and VDOS. For these properties we compare the results obtained from classical MD and thermostatted ring polymer molecular dynamics (TRPMD). For these properties, since real time quantum dynamics is intractable for such a large atomistic condensed phase system for the timescales required to compute these properties, we use TRPMD to approximate the role of NQEs. TRPMD has previously been shown to be an accurate way for treating NQEs in the dynamics of condensed phase systems, however it is known to spuriously broaden high-frequency vibrational modes.<sup>38,61</sup>

	AFQMC	CCSD(T)	CCSD
Classical T=300K			
$(10^{-9} \text{ m}^2/\text{s})$	2.09 (0.05)	2.21 (0.06)	2.60 (0.08)
TRPMD T=300K			
$(10^{-9} \text{ m}^2/\text{s})$	2.16 (0.09)	2.30 (0.08)	2.80 (0.11)
TRPMD T=370K			
$(10^{-9} \text{ m}^2/\text{s})$	7.09 (0.11)	8.16 (0.14)	8.29 (0.14)

TABLE I. Diffusion coefficients for liquid water when running classical and TRPMD simulations using NNPs fitted to either CCSD, CCSD(T), and AFQMC energies at both 300K and 370K. Mean diffusion coefficients and standard errors of the mean are reported and are calculated using 20 ps length trajectories taken from 1 ns classical MD or 500 ps TRPMD trajectories. The experimental diffusion coefficient for water at 300 K and 370 K are  $2.41\pm0.05^{59}$  and  $8.26\pm0.02$   $(10^{-9} \text{ m}^2/\text{s})$ ,  $^{60}$  respectively.

The diffusion coefficients obtained for the three correlated methods are shown in Table I at 300 K and 370 K. Unlike the other properties we report, diffusion coefficients exhibit a notable scaling with system size that must be corrected for to make comparisons with experiment. Hence, as described in SI Sec. IV A, the diffusion coefficients were computed using simulations of 64 water molecules and then extrapolated to the infinite system size limit using the previously derived system size scaling relation<sup>62</sup> and the experimental viscosity of water. 63 At 300 K, where the experimentally measured diffusion coefficient is  $2.41\pm0.05\times10^{-9}$  m<sup>2</sup>/s,<sup>59</sup> when classical MD is used AFQMC and CCSD(T) yield smaller diffusion coefficients than observed experimentally,  $2.09\pm0.05$ and  $2.21\pm0.06 \times 10^{-9}$  m<sup>2</sup>/s respectively, while CCSD gives a larger value  $2.60\pm0.08 \times 10^{-9}$  m<sup>2</sup>/s. This behavior is consistent with the trends observed for the electronic structure approaches in the structural properties, where CCSD formed a slightly understructured hydrogen bond network compared to the more accurate correlated methods, which here leads to faster dynamics. Upon including NQEs using TRPMD, the diffusion coefficients for all three electronic methods increase, consistent with the disruption of the hydrogen bond network upon including zero-point energy, which brings the CCSD(T) result  $(2.30\pm0.08 \times 10^{-9} \text{ m}^2/\text{s})$  to within the statistical error bar of the experimentally observed value. Even with NQEs included the AFQMC diffusion coefficient is lower  $(2.16\pm0.09 \times 10^{-9} \text{ m}^2/\text{s})$  than experiment, consistent with it forming a more structured liquid. However, it should be noted that the discrepancy in the diffusion coefficient is very small; to change water's diffusion coefficient from that observed at 300 K via classical MD using our CCSD(T) model to the value obtained by performing TRPMD dynamics would require less than a 2 K change in the temperature of the liquid. 60 In addition, for dynamical properties TRPMD only approximately includes NQEs and hence the better agreement of CCSD(T) with the experimental value could be changed if a different approach was used to treat the quantum dynamics of the nuclei. At 370 K, when TRPMD is used CCSD and CCSD(T) give similar results  $(8.29\pm0.14 \text{ and } 8.16\pm0.14\times10^{-9} \text{ m}^2/\text{s}, \text{ re-}$ spectively), both of which are close to the experimental value

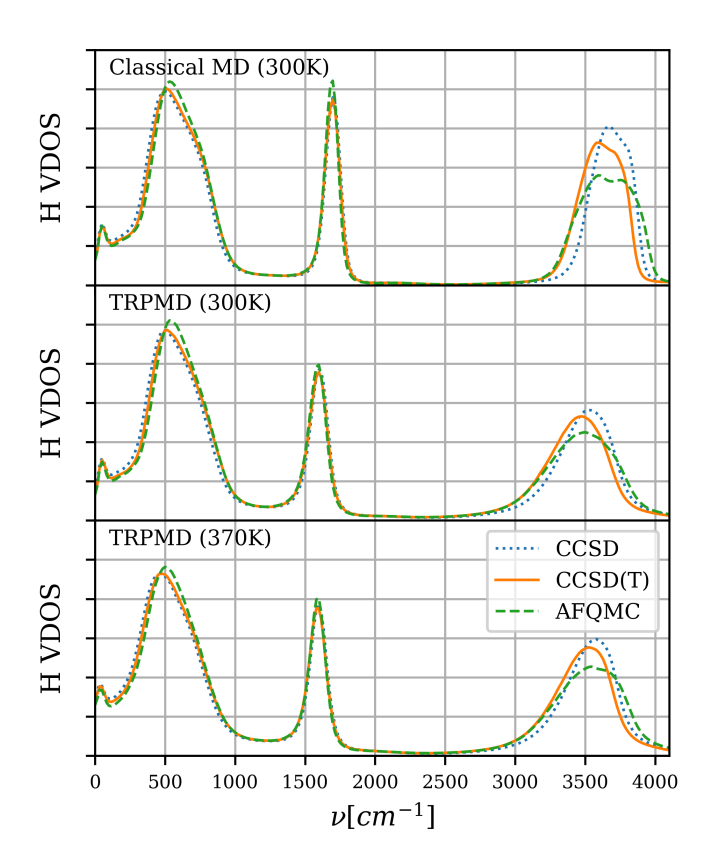


FIG. 3. The hydrogen VDOS for liquid water when running classical and TRPMD simulations using NNPs fitted to either CCSD, CCSD(T), and AFQMC energies at both 300K and 370K.

of  $8.26\pm0.02\times10^{-9}$  m<sup>2</sup>/s.<sup>60</sup> The diffusion of AFQMC water is again considerably slower, which is consistent with the relatively greater degree of structure we saw in the latter's respective oxygen-oxygen RDF and q distribution.

The VDOS in Figure 3 provides more information on the frequency dependence of the dynamics of water for the three electronic structure methods, since the diffusion coefficient is simply proportional to its zero frequency limit. All three methods give qualitatively similar VDOS around the lower frequency librational band (~500 cm<sup>-1</sup>) and peak associated with the H-O-H bending mode (~1600 cm<sup>-1</sup>). At 300 K using classical MD, the main qualitative difference lies in the OH stretch peak (3000-4000 cm<sup>-1</sup>), with CCSD(T) giving a peak that is redshifted by ~80 cm<sup>-1</sup> with respect to the CCSD peak, while the AFQMC peak is slightly broader than the others and is centered closer to the CCSD result. At the low-frequency end of the O-H stretch peak, the VDOS for CCSD(T) and AFQMC coincide with one another. Low frequency O-H stretches are typically associated with stronger hydrogen bonds and the frequency of the O-H stretch peak has previously been demonstrated to be inversely correlated with the tetrahedrality parameter.<sup>5</sup> Hence, the consistency between CCSD(T) and AFQMC at the low frequency part of their respective O-H stretch peaks is consistent with the structural evidence in Sec. III A showing that these two methods similarly structure water via slightly stronger hydrogen bonds as compared to CCSD. The TRPMD simulations at 300 K, which include NOEs via TRPMD simulations, lead to a ~120 cm<sup>-1</sup> red-shift and broadening of the stretch peak and a ~100 cm<sup>-1</sup> shift in the bend for all three methods, which is consistent with observations from previous studies. 38,61 Although some of the broadening likely arises from physical effects, TRPMD is known to introduce spurious broadening of high-frequency vibrational modes.<sup>38,61</sup> At 370 K the most significant difference is the shift in the zero frequency intensity, which we expect since this is directly related to the self-diffusion coefficient and otherwise the VDOS is qualitatively similar with respect to the 300 K results. This is expected since for the high frequency modes the zero point energy greatly exceeds the thermal energy in the the mode, i.e.  $k_BT \ll \hbar\omega/2$  where  $k_B$  is the Boltzmann constant, T is the temperature and  $\omega$  is the frequency of the mode.

Overall, the trends we observe in the dynamical properties largely mirror the evidence we presented for the structural properties showing that CCSD results in an understructured description of liquid water at 300 K, as compared to CCSD(T) and AFQMC, while at 300 K and 370 K AFQMC overstructures water. The differences in the diffusion coefficients in Table I reflect this trend, with CCSD overestimating the experimental diffusion coefficient at 300 K with its understructured description of water and AFQMC underpredicting the diffusion coefficient at 370 K. With the VDOS the main differences between the three correlated methods manifest in the O-H stretch peak positions and breadth, with peaks given by MD at 300 K for both CCSD(T) and AFQMC skewed more to lower frequencies that are associated with stronger hydrogen bonds.

Finally, in SI Figs. 15-22 we compare the results obtained using our MLPs for CCSD, CCSD(T), and AFOMC to the MB-Pol model and revPBE0-D3. While the RDFs obtained for all closely match, in the VDOS we observe that MB-Pol has an OH stretch band that is narrower and slightly blueshifted when compared to CCSD(T) and AFQMC, and which is more similar to that obtained from CCSD. MB-Pol, which was fit to calculations on gas phase dimers and trimers at the CCSD(T) level of electronic structure, <sup>15–18</sup> also gives stronger agreement with the CCSD results for the tetrahedrality distribution which is consistent with the stronger correlation of its energies with CCSD (0.873) than CCSD(T) (0.852) in SI Fig. 2. revPBE0-D3 also possesses a hydrogen VDOS with an OH stretch band that is narrow and blue-shifted like that of MB-Pol and CCSD, but has a tetrahedrality distribution in closer agreement with that of CCSD(T) and AFQMC.

## IV. CONCLUSION

In summary, we leveraged developments in high-level periodic electronic structure theory and exploited methods to improve the data efficiency of fitting MLPs to investigate the structural and dynamical properties of liquid water at the level of CCSD, CCSD(T), and AFQMC. We devised a data efficient protocol for training MLPs that uses small periodic boxes of

water (16 molecules) sampled judiciously via an iterative QbC active learning procedure. To make the most out of the few configuration energies we can afford to compute, we also employed a transfer learning approach that leverages the transferability of physics between lower level electronic structure methods (e.g. DFT with the BLYP functional, revPBE0-D3 functional, or HF) and our target higher-level methods, using MLPs fit to the former to initialize a fine-tuning transfer learning fit to the latter. Using this approach we showed that we can train stable MLPs with as few as 50 configuration energies, capture the RDFs with 100 (SI Fig. 4), and with 200 configuration energies obtain both accurate structural and dynamical properties such as the diffusion constant and VDOS (SI Fig. 9). In contrast, with these same 200 energies we were unable to train stable models using delta learning or using random initialization of the model.

We used our MLPs trained to CCSD, CCSD(T), and AFQMC to examine how different structural and dynamical properties of liquid water are affected by the level of dynamic electron correlation accounted for and the inclusion of NOEs. Our results indicate that CCSD tends to understructure liquid water and overpredict the diffusion coefficient, as compared to experiment. On the other hand, both CCSD(T) and AFQMC give oxygen-oxygen RDFs and diffusion coefficients that are more consistent with experimental values at 300 K, suggesting that the more accurate treatment of dynamical correlation present in these methods is sufficient for describing liquid water. The inclusion of NQEs for our 300 K simulations bring the CCSD(T) and AFQMC results in even closer agreement with experiment and seems to generally manifest as a slight destructuring of liquid water for all three electronic structure descriptions. This small destructuring upon including NQEs for these correlated methods is in contrast to some DFT exchange correlation functionals where due to the overprediction of the anharmonicity of the O-H coordinate the inclusion of NQEs works to structure the liquid phase.<sup>38</sup>

Ultimately, we envision that the configurations and energies that form the training dataset, the resulting MLPs, and the protocols we employed here will be useful in their own separate respects for future work in modeling potential energy surfaces for condensed phase systems.

#### **ACKNOWLEDGMENTS**

T.E.M and M.S.C were supported by the National Science Foundation under Grant No. CHE-2154291. This research also used resources of the National Energy Research Scientific Computing Center (NERSC), a U.S. Department of Energy Office of Science User Facility operated under Contract No. DE-AC02-05CH11231. This work was also supported by the US Air Force Office of Scientific Research under Grant No. FA9550-21-1-0400 (H.-Z.Y. and T.C.B.). We acknowledge the computing resources provided by Columbia University's Shared Research Computing Facility project, which is supported by NIH Research Facility Improvement Grant No. 1G20RR030893-01, and associated funds from the New York State Empire State Development, Division of Science Tech-

nology and Innovation (NYSTAR) Contract No. C090171, both awarded April 15, 2010. The Flatiron Institute is a division of the Simons Foundation.

#### ASSOCIATED CONTENT

The Supporting Information is available free of charge via the Internet at http://pubs.acs.org.

Additional details for the the electronic structure calculations, training of machine learning models, molecular dynamics simulations, and the calculation of diffusion coefficients and vibrational density of states. Benchmarks for the transferability of relative training set performance, transfer learning procedure, and the effect of stochastic error in the AFQMC energies. Comparison of results when different electronic structure methods are used to initialize the transfer learning procedure. Comparison of results with MB-Pol and revPBE0-D3.

Datasets used to train our MLPs (HF, BLYP, revPBE0-D3, CCSD, CCSD(T), and AFQMC). Weights for our CCSD, CCSD(T), and AFQMC committee MLPs. The datasets and weights for the MLPs shared here are in formats specific to the n2p2 package, v2.1.0.<sup>64</sup>

<sup>1</sup>DiStasio, R. A.; Santra, B.; Li, Z.; Wu, X.; Car, R. The individual and collective effects of exact exchange and dispersion interactions on the ab initio structure of liquid water. *The Journal of Chemical Physics* **2014**, *141*, 084502.

<sup>2</sup>Gillan, M. J.; Alfè, D.; Michaelides, A. Perspective: How good is DFT for water? *Journal of Chemical Physics* **2016**, *144*.

<sup>3</sup>Del Ben, M.; Schönherr, M.; Hutter, J.; Vandevondele, J. Bulk liquid water at ambient temperature and pressure from mp2 theory. *The Journal of Physical Chemistry Letters* **2013**, *4*, 3753–3759.

<sup>4</sup>Morawietz, T.; Singraber, A.; Dellago, C.; Behler, J. How van der Waals interactions determine the unique properties of water. *Proceedings of the National Academy of Sciences* **2016**, *113*, 8368–8373.

<sup>5</sup>Morawietz, T.; Marsalek, O.; Pattenaude, S. R.; Streacker, L. M.; Ben-Amotz, D.; Markland, T. E. The Interplay of Structure and Dynamics in the Raman Spectrum of Liquid Water over the Full Frequency and Temperature Range. *The Journal of Physical Chemistry Letters* **2018**, *9*, 851–857.

<sup>6</sup>Zhang, L.; Han, J.; Wang, H.; Car, R.; E, W. Deep Potential Molecular Dynamics: A Scalable Model with the Accuracy of Quantum Mechanics. *Phys. Rev. Lett.* **2018**, *120*, 143001.

<sup>7</sup>Cheng, B.; Engel, E. A.; Behler, J.; Dellago, C.; Ceriotti, M. Ab initio thermodynamics of liquid and solid water. *Proceedings of the National Academy of Sciences* **2019**, *116*, 1110–1115.

<sup>8</sup>Schran, C.; Brezina, K.; Marsalek, O. Committee neural network potentials control generalization errors and enable active learning. *The Journal of Chemical Physics* **2020**, *153*, 104105.

<sup>9</sup>Yao, Y.; Kanai, Y. Temperature dependence of nuclear quantum effects on liquid water via artificial neural network model based on SCAN meta-GGA functional. *The Journal of Chemical Physics* **2020**, *153*, 044114.

<sup>10</sup>Zhang, C.; Tang, F.; Chen, M.; Xu, J.; Zhang, L.; Qiu, D. Y.; Perdew, J. P.; Klein, M. L.; Wu, X. Modeling Liquid Water by Climbing up Jacob's Ladder in Density Functional Theory Facilitated by Using Deep Neural Network Potentials. *The Journal of Physical Chemistry B* **2021**, *125*, 11444–11456. PMID: 34533960.

<sup>11</sup>Yao, Y.; Kanai, Y. Nuclear Quantum Effect and Its Temperature Dependence in Liquid Water from Random Phase Approximation via Artificial Neural Network. *The Journal of Physical Chemistry Letters* **2021**, *12*, 6354–6362.

<sup>12</sup>Lan, J.; Wilkins, D. M.; Rybkin, V.; Iannuzzi, M.; Hutter, J. Quantum Dynamics of Water from Møller-Plesset Perturbation Theory via a Neural Network Potential. *chemRxiv* 2021, DOI: 10.26434/chemrxiv-2021-n32q8-y2

- <sup>13</sup>Liu, J.; Lan, J.; He, X. Toward High-level Machine Learning Potential for Water Based on Quantum Fragmentation and Neural Networks. *The Jour*nal of Physical Chemistry A 2022, 126, 3926–3936, PMID: 35679610.
- <sup>14</sup>Bukowski, R.; Szalewicz, K.; Groenenboom, G. C.; van der Avoird, A. Predictions of the Properties of Water from First Principles. *Science* 2007, 315, 1249–1252.
- <sup>15</sup>Babin, V.; Leforestier, C.; Paesani, F. Development of a "First Principles" Water Potential with Flexible Monomers: Dimer Potential Energy Surface, VRT Spectrum, and Second Virial Coefficient. *Journal of Chemical Theory and Computation* **2013**, *9*, 5395–5403, PMID: 26592277.
- <sup>16</sup>Babin, V.; Medders, G. R.; Paesani, F. Development of a "First Principles" Water Potential with Flexible Monomers. II: Trimer Potential Energy Surface, Third Virial Coefficient, and Small Clusters. *Journal of Chemical Theory and Computation* **2014**, *10*, 1599–1607, PMID: 26580372.
- <sup>17</sup> Medders, G. R.; Babin, V.; Paesani, F. Development of a "First-Principles" Water Potential with Flexible Monomers. III. Liquid Phase Properties. *Journal of Chemical Theory and Computation* **2014**, *10*, 2906–2910, PMID: 26588266
- <sup>18</sup>Reddy, S. K.; Straight, S. C.; Bajaj, P.; Huy Pham, C.; Riera, M.; Moberg, D. R.; Morales, M. A.; Knight, C.; Götz, A. W.; Paesani, F. On the accuracy of the MB-pol many-body potential for water: Interaction energies, vibrational frequencies, and classical thermodynamic and dynamical properties from clusters to liquid water and ice. *The Journal of Chemical Physics* 2016, 145, 194504.
- <sup>19</sup>Schran, C.; Behler, J.; Marx, D. Automated Fitting of Neural Network Potentials at Coupled Cluster Accuracy: Protonated Water Clusters as Testing Ground. *Journal of Chemical Theory and Computation* 2020, 16, 88–99.
- <sup>20</sup>Nandi, A.; Qu, C.; Houston, P. L.; Conte, R.; Yu, Q.; Bowman, J. M. A CCSD(T)-Based 4-Body Potential for Water. *The Journal of Physical Chemistry Letters* **2021**, *12*, 10318–10324.
- <sup>21</sup> Yu, Q.; Qu, C.; Houston, P. L.; Conte, R.; Nandi, A.; Bowman, J. M. q-AQUA: A Many-Body CCSD(T) Water Potential, Including Four-Body Interactions, Demonstrates the Quantum Nature of Water from Clusters to the Liquid Phase. *The Journal of Physical Chemistry Letters* 2022, *13*, 5068–5074, PMID: 35652912.
- <sup>22</sup>Bowman, J. M.; Qu, C.; Conte, R.; Nandi, A.; Houston, P. L.; Yu, Q. Δ-Machine Learned Potential Energy Surfaces and Force Fields. *Journal of Chemical Theory and Computation* **2023**, *19*, 1–17, PMID: 36527383.
- <sup>23</sup> Daru, J.; Forbert, H.; Behler, J.; Marx, D. Coupled Cluster Molecular Dynamics of Condensed Phase Systems Enabled by Machine Learning Potentials: Liquid Water Benchmark. *Phys. Rev. Lett.* **2022**, *129*, 226001.
- <sup>24</sup>Archibald, R.; Krogel, J. T.; Kent, P. R. Gaussian process based optimization of molecular geometries using statistically sampled energy surfaces from quantum Monte Carlo. *Journal of Chemical Physics* 2018, 149.
- <sup>25</sup>Ryczko, K.; Krogel, J. T.; Tamblyn, I. Machine Learning Diffusion Monte Carlo Energies. *Journal of Chemical Theory and Computation* **2022**, *18*, 7695–7701, PMID: 36317712.
- <sup>26</sup>Huang, C.; Rubenstein, B. M. Machine Learning Diffusion Monte Carlo Forces. *The Journal of Physical Chemistry A* **2023**, *127*, 339–355, PMID: 36576803.
- <sup>27</sup>Burnham, C. J.; Anick, D. J.; Mankoo, P. K.; Reiter, G. F. The vibrational proton potential in bulk liquid water and ice. *The Journal of Chemical Physics* **2008**, *128*, 154519.
- <sup>28</sup>Purvis, G. D.; Bartlett, R. J. A full coupled-cluster singles and doubles model: The inclusion of disconnected triples. *The Journal of Chemical Physics* 1982, 76, 1910–1918.
- <sup>29</sup>Raghavachari, K.; Trucks, G. W.; Pople, J. A.; Head-Gordon, M. A fifth-order perturbation comparison of electron correlation theories. *Chemical Physics Letters* **1989**, *157*, 479–483.
- <sup>30</sup>Zhang, S.; Krakauer, H. Quantum Monte Carlo Method using Phase-Free Random Walks with Slater Determinants. *Phys. Rev. Lett.* **2003**, *90*, 136401
- <sup>31</sup>Seung, H. S.; Oppert, M.; Sompolinsky, H. Query by committee. Proceedings of the fifth annual workshop on Computational learning theory (COLT '92). New York, 1992; pp 287–294.
- <sup>32</sup>Krogh, A.; Vedelsby, J. Neural Network Ensembles, Cross Validation, and Active Learning. Advances in Neural Information Processing Systems. 1994; pp 231–238.
- <sup>33</sup>Behler, J.; Parrinello, M. Generalized Neural-Network Representation of High-Dimensional Potential-Energy Surfaces. *Phys. Rev. Lett.* 2007, 98,

- 146401
- <sup>34</sup>Elstner, M.; Porezag, D.; Jungnickel, G.; Elsner, J.; Haugk, M.; Frauenheim, T.; Suhai, S.; Seifert, G. Self-consistent-charge density-functional tight-binding method for simulations of complex materials properties. *Phys. Rev. B* **1998**, *58*, 7260–7268.
- <sup>35</sup>Perdew, J. P.; Burke, K.; Ernzerhof, M. Generalized Gradient Approximation Made Simple. *Phys. Rev. Lett.* 1996, 77, 3865–3868.
- <sup>36</sup>Zhang, Y.; Yang, W. Comment on "Generalized Gradient Approximation Made Simple". Phys. Rev. Lett. 1998, 80, 890–890.
- <sup>37</sup>Adamo, C.; Barone, V. Toward reliable density functional methods without adjustable parameters: The PBE0 model. *The Journal of Chemical Physics* 1999, 110, 6158–6170.
- <sup>38</sup>Marsalek, O.; Markland, T. E. Quantum Dynamics and Spectroscopy of Ab Initio Liquid Water: The Interplay of Nuclear and Electronic Quantum Effects. *The Journal of Physical Chemistry Letters* 2017, 8, 1545–1551.
- <sup>39</sup>Becke, A. D. Density-functional exchange-energy approximation with correct asymptotic behavior. *Phys. Rev. A* 1988, 38, 3098–3100.
- <sup>40</sup>Lee, C.; Yang, W.; Parr, R. G. Development of the Colle-Salvetti correlation-energy formula into a functional of the electron density. *Phys. Rev. B* **1988**, *37*, 785–789.
- <sup>41</sup>Kühne, T. D.; Krack, M.; Parrinello, M. Static and Dynamical Properties of Liquid Water from First Principles by a Novel Car-Parrinello-like Approach. *Journal of Chemical Theory and Computation* **2009**, *5*, 235–241, PMID: 26610101.
- <sup>42</sup>Pan, S. J.; Yang, Q. A Survey on Transfer Learning. *IEEE Transactions on Knowledge and Data Engineering* 2010, 22, 1345–1359.
- <sup>43</sup>Singraber, A.; Morawietz, T.; Behler, J.; Dellago, C. Parallel Multistream Training of High-Dimensional Neural Network Potentials. *Journal* of Chemical Theory and Computation 2019, 15, 3075–3092.
- <sup>44</sup>Sun, Q.; Zhang, X.; Banerjee, S.; Bao, P.; Barbry, M.; Blunt, N. S.; Bogdanov, N. A.; Booth, G. H.; Chen, J.; Cui, Z.-H.; Eriksen, J. J.; Gao, Y.; Guo, S.; Hermann, J.; Hermes, M. R.; Koh, K.; Koval, P.; Lehtola, S.; Li, Z.; Liu, J.; Mardirossian, N.; McClain, J. D.; Motta, M.; Mussard, B.; Pham, H. Q.; Pulkin, A.; Purwanto, W.; Robinson, P. J.; Ronca, E.; Sayfutyarova, E. R.; Scheurer, M.; Schurkus, H. F.; Smith, J. E. T.; Sun, C.; Sun, S.-N.; Upadhyay, S.; Wagner, L. K.; Wang, X.; White, A.; Whitfield, J. D.; Williamson, M. J.; Wouters, S.; Yang, J.; Yu, J. M.; Zhu, T.; Berkelbach, T. C.; Sharma, S.; Sokolov, A. Y.; Chan, G. K.-L. Recent developments in the PySCF program package. *The Journal of Chemical Physics* 2020, *153*, 024109.
- <sup>45</sup>McClain, J.; Sun, Q.; Chan, G. K.-L.; Berkelbach, T. C. Gaussian-Based Coupled-Cluster Theory for the Ground-State and Band Structure of Solids. *Journal of Chemical Theory and Computation* 2017, 13, 1209–1218, PMID: 28218843.
- <sup>46</sup>Ye, H.-Z.; Berkelbach, T. C. Fast periodic Gaussian density fitting by range separation. J. Chem. Phys. 2021, 154, 131104.
- <sup>47</sup>Ye\*, H.-Z.; Berkelbach, T. C. Tight distance-dependent estimators for screening two-center and three-center short-range Coulomb integrals over Gaussian basis functions. *J. Chem. Phys.* **2021**, *155*, 124106.
- <sup>48</sup>Kim, J.; Baczewski, A. D.; Beaudet, T. D.; Benali, A.; Bennett, M. C.; Berrill, M. A.; Blunt, N. S.; Borda, E. J. L.; Casula, M.; Ceperley, D. M.; Chiesa, S.; Clark, B. K.; Clay, R. C.; Delaney, K. T.; Dewing, M.; Esler, K. P.; Hao, H.; Heinonen, O.; Kent, P. R. C.; Krogel, J. T.; Kylänpää, I.; Li, Y. W.; Lopez, M. G.; Luo, Y.; Malone, F. D.; Martin, R. M.; Mathuriya, A.; McMinis, J.; Melton, C. A.; Mitas, L.; Morales, M. A.; Neuscamman, E.; Parker, W. D.; Flores, S. D. P.; Romero, N. A.; Rubenstein, B. M.; Shea, J. A. R.; Shin, H.; Shulenburger, L.; Tillack, A. F.; Townsend, J. P.; Tubman, N. M.; Goetz, B. V. D.; Vincent, J. E.; Yang, D. C.; Yang, Y.; Zhang, S.; Zhao, L. QMCPACK: an open source ab initio quantum Monte Carlo package for the electronic structure of atoms, molecules and solids. *Journal of Physics: Condensed Matter* 2018, *30*, 195901.
- <sup>49</sup>Kent, P. R. C.; Annaberdiyev, A.; Benali, A.; Bennett, M. C.; Landinez Borda, E. J.; Doak, P.; Hao, H.; Jordan, K. D.; Krogel, J. T.; Kylänpää, I.; Lee, J.; Luo, Y.; Malone, F. D.; Melton, C. A.; Mitas, L.; Morales, M. A.; Neuscamman, E.; Reboredo, F. A.; Rubenstein, B.; Saritas, K.; Upadhyay, S.; Wang, G.; Zhang, S.; Zhao, L. QMCPACK: Advances in the development, efficiency, and application of auxiliary field and real-space variational and diffusion quantum Monte Carlo. *J. Chem. Phys.* 2020, 152, 174105
- <sup>50</sup>Malone, F. D.; Mahajan, A.; Spencer, J. S.; Lee, J. ipie: A Python-Based

- Auxiliary-Field Quantum Monte Carlo Program with Flexibility and Efficiency on CPUs and GPUs. *Journal of Chemical Theory and Computation* **2023**, *19*, 109–121, PMID: 36503227.
- <sup>51</sup>Lee, J.; Pham, H. Q.; Reichman, D. R. Twenty Years of Auxiliary-Field Quantum Monte Carlo in Quantum Chemistry: An Overview and Assessment on Main Group Chemistry and Bond-Breaking. *J. Chem. Theory Com*put. 2022, 2022.
- <sup>52</sup>Čířek, J. On the Correlation Problem in Atomic and Molecular Systems. Calculation of Wavefunction Components in Ursell-Type Expansion Using Quantum-Field Theoretical Methods. *The Journal of Chemical Physics* 1966, 45, 4256–4266.
- <sup>53</sup>Taube, A. G.; Bartlett, R. J. Frozen natural orbital coupled-cluster theory: Forces and application to decomposition of nitroethane. *J. Chem. Phys.* 2008, 128, 164101.
- <sup>54</sup>Lange, M. F.; Berkelbach, T. C. Active space approaches combining coupled-cluster and perturbation theory for ground states and excited states. *Mol. Phys.* **2020**, *118*, e1808726.
- <sup>55</sup>Skinner, L. B.; Huang, C.; Schlesinger, D.; Pettersson, L. G. M.; Nilsson, A.; Benmore, C. J. Benchmark oxygen-oxygen pair-distribution function of ambient water from x-ray diffraction measurements with a wide Q-range. *The Journal of Chemical Physics* **2013**, *138*, 074506.
- <sup>56</sup>Mariedahl, D.; Perakis, F.; Späh, A.; Pathak, H.; Kim, K. H.; Camisasca, G.; Schlesinger, D.; Benmore, C.; Pettersson, L. G. M.; Nilsson, A.; Amann-Winkel, K. X-ray Scattering and O-O Pair-Distribution Functions of Amorphous Ices. *The Journal of Physical Chemistry B* 2018, 122, 7616–7624.

- <sup>57</sup>Jeffrey R. Errington,; Pablo G. Debenedetti, Relationship between structural order and the anomalies of liquid water. *Nature* **2001**, *409*, 318.
- <sup>58</sup>Habershon, S.; Markland, T. E.; Manolopoulos, D. E. Competing quantum effects in the dynamics of a flexible water model. *The Journal of Chemical Physics* 2009, *131*, 024501.
- <sup>59</sup>Holz, M.; Heil, S. R.; Sacco, A. Temperature-dependent self-diffusion coefficients of water and six selected molecular liquids for calibration in accurate 1H NMR PFG measurements. *Phys. Chem. Chem. Phys.* **2000**, 2, 4740–4742.
- <sup>60</sup>Dietrich, O. Diffusion Coefficients of Water. https://dtrx.de/od/diff/, 2002; [Accessed: 30-August-2022].
- <sup>61</sup>Rossi, M.; Liu, H.; Paesani, F.; Bowman, J.; Ceriotti, M. Communication: On the consistency of approximate quantum dynamics simulation methods for vibrational spectra in the condensed phase. *The Journal of Chemical Physics* **2014**, *141*, 181101.
- <sup>62</sup>Yeh, I. C.; Hummer, G. System-size dependence of diffusion coefficients and viscosities from molecular dynamics simulations with periodic boundary conditions. *The Journal of Physical Chemistry B* **2004**, *108*, 15873– 15879
- <sup>63</sup>Kestin, J.; Sokolov, M.; Wakeham, W. A. Viscosity of liquid water in the range -8C to 150C. *Journal of Physical and Chemical Reference Data* 1978, 7, 941–948.
- <sup>64</sup>Singraber, Andreas, n2p2 The neural network potential package. https://compphysvienna.github.io/n2p2/.